THE JOURNAL OF BIOLOGICAL CHEMISTRY VOL. 291, NO. 20, pp. 10541–10550, May 13, 2016

Different Roles of Negative and Positive Components of the Circadian Clock in Oncogene-induced Neoplastic Transformation*[S]

Received for publication, November 30, 2015, and in revised form, March 7, 2016 Published, JBC Papers in Press, March 9, 2016, DOI 10.1074/jbc.M115.706481

Chiharu Katamune[‡1], Satoru Koyanagi[§1], Shoya Shiromizu[‡], Naoya Matsunaga[‡], Shigeki Shimba[¶], Shigenobu Shibata[‖], and Shigehiro Ohdo[‡2]

From the [‡]Department of Pharmaceutics and [§]Department of Glocal Healthcare Science, Faculty of Pharmaceutical Sciences, Kyushu University, Fukuoka 812-8582, Japan, [¶]Department of Health Science, School of Pharmacy, Nihon University, Funabashi 274-8555, Japan, and [‖]Laboratory of Physiology and Pharmacology, School of Advanced Science and Engineering, Waseda University Tokyo, 162-0056, Japan

In mammals, circadian rhythms in physiological function are generated by a molecular oscillator driven by transcriptional-translational feedback loop consisting of negative and positive regulators. Disruption of this circadian clock machinery is thought to increase the risk of cancer development, but the potential contributions of each component of circadian clock to oncogenesis have been little explored. Here we reported that negative and positive transcriptional regulators of circadian feedback loop had different roles in oncogene-induced neoplastic transformation. Mouse embryonic fibroblasts prepared from animals deficient in negative circadian clock regulators, *Period2* (*Per2*) or *Cryptochrome1/2* (*Cry1/2*), were prone to transformation induced by co-expression of H-ras^{V12} and SV40 large T antigen (SV40LT). In contrast, mouse embryonic fibroblasts prepared from mice deficient in positive circadian clock regulators, *Bmal1* or *Clock*, showed resistance to oncogene-induced transformation. In *Per2* mutant and *Cry1/2*-null cells, the introduction of oncogenes induced expression of ATF4, a potent repressor of cell senescence-associated proteins p16INK4a and p19ARF. Elevated levels of ATF4 were sufficient to suppress expression of these proteins and drive oncogenic transformation. Conversely, in *Bmal1*-null and *Clock* mutant cells, the expression of ATF4 was not induced by oncogene introduction, which allowed constitutive expression of p16INK4a and p19ARF triggering cellular senescence. Although genetic ablation of either negative or positive transcriptional regulators of the circadian clock leads to disrupted rhythms in physiological functions, our findings define their different contributions to neoplastic cellular transformation.

The circadian clock is a timekeeping system that allows organisms to adapt their physiological and behavioral functions to anticipatory changes in their environment. In mammals, the circadian clock system is hierarchically organized, consisting of a light-responsive central clock in the suprachiasmatic nuclei of the anterior hypothalamus and subsidiary clocks in other brain regions and peripheral tissues (1). The suprachiasmatic nuclei entrains and synchronizes subsidiary clocks with the environmental light-dark cycle, whereas peripheral clocks regulate tissue-specific functions in an anticipatory manner.

Central and peripheral clocks are both governed by interconnected transcriptional and translational feedback loops (2). The gene products of *Bmal1* (also known as *Arntl*) and *Clock* form a heterodimer that activates the transcription of *Period* (*Per*) and *Cryptochrome* (*Cry*) genes. Once PER and CRY proteins have reached a critical concentration, they attenuate BMAL1/CLOCK-mediated transactivation. The alternating activation and suppression of the BMAL1/CLOCK-driven positive loop and PER/CRY-controlled negative loop result in a circadian oscillation in the molecular clock and also regulate 24-h variations in output physiology through the periodic activation/repression of clock-controlled genes (3, 4).

Because the expression of up to 10% of genes has been suggested to be under the control of the circadian clock (5), it should not come as a surprise that disruptions in the circadian clock system lead to the onset of various diseases. In fact, several epidemiological analyses and laboratory animal studies also revealed a relationship between disruptions in circadian rhythms and cancer development. For example, human night shift workers are at an increased risk of developing breast, prostate, colon, and endometrial cancers as well as hepatocellular carcinoma and non-Hodgkin lymphoma (6–7). These epidemiological findings are also supported by animal studies in which repetitive changes in the light-dark cycle facilitate the growth of implanted tumors (8, 9). Furthermore, spontaneous as well as radiation-induced tumor development is enhanced in circadian gene-defective animals whose behavioral and physiological rhythms are abnormal phenotypes (10, 11).

Although genetic ablation of either negative or positive transcriptional regulators of the circadian feedback loop leads to disruption of the rhythms in physiological functions (1, 2), the potential contributions of each circadian clock regulator to oncogenesis have been little explored. In this study we found that negative and positive components of circadian feedback

* This work was supported in part of Japan Society for the Promotion of Science (JSPS) KAKENHI Grants FCG6670317 (to S. K.) and 25253038 (to S. O.) and the Mandom International Research Grants on Alternative to Animal Experiments. The authors declare that they have no conflicts of interest with the contents of this article.
[S] This article contains supplemental Fig. S1.
[1] Both authors contributed equally to this work.
[2] To whom correspondence should be addressed: Dept. of Pharmaceutics, Faculty of Pharmaceutical Sciences, Kyushu University, 3-1-1 Maidashi Higashi-ku, Fukuoka 812-8582, Japan. Tel.: 81-92-642-6610; Fax: 81-92-642-6614; E-mail: ohdo@phar.kyushu-u.ac.jp.

loop played different roles during oncogene-induced neoplastic transformation. Mouse embryonic fibroblasts (MEFs)[3] prepared from *Per2* mutant (*Per2*$^{m/m}$) or *Cry1/2*-null (*Cry1/2*$^{-/-}$) mice were prone to oncogenic transformation induced by coexpression of H-ras^{V12} and SV40 large T antigen (SV40LT); however, these oncogene induced expression of cellular senescence-associated proteins in *Bmal1*-null (*Bmal1*$^{-/-}$) or *Clock* mutant (*Clk*/*Clk*) cells, resulting in failure of their neoplastic transformation. Because the expression of ATF4, a potent repressor of cell senescence-associated proteins, was altered in oncogene-introduced clock gene-defective cells, we further focused on this gene to investigate the roles of negative and positive components of the circadian clock in the neoplastic transformation of mouse fibroblasts.

Experimental Procedures

Treatments of Animals and Cells—*Per2*$^{m/m}$, *Bmal1*$^{-/-}$, and *Clock* mutant (*Clk/Clk*) mice with an ICR background and wild type mice of the same strain were housed in a temperature-controlled (24 ± 1 °C) room under a 12-h light:12-h dark cycle. MEFs were prepared by standard techniques (12) from littermate embryos of *Per2*$^{m/m}$, *Bmal1*$^{-/-}$, *Clk/Clk*, or wild-type mice, and cells were maintained in Dulbecco's modified Eagle's medium (DMEM, Sigma) supplemented with 10% fetal bovine serum (FBS). *Cry*-null MEFs, defective in both *Cry1* and *Cry2*, were kindly provided by Dr. Ueda (13). The preparation of MEFs from each genotype was conducted at least three times. Cells were expanded for three or four passages before the experiments. To achieve oncogenic transformation, MEFs were infected with 1×10^6 colony-forming units/ml retroviral vectors expressing H-ras^{V12} and SV40LT (14). Plasmid vectors (pcDNA3.1; Invitrogen) expressing *Per2*, *Bmal1*, or *Atf4* were also transfected into oncogene-introduced MEFs. Transgene-expressing cells were selected with G418 (Wako, Osaka, Japan), and individual colonies were expanded and maintained in media containing 4 μg/ml G418.

Male NOD-SCID mice were purchased from Charles River. They were inoculated with oncogenic-transformed MEFs (5×10^6 cells/mouse). Tumor volumes were measured by caliper, and values were obtained by multiplying the square of the smallest diameter with the largest diameter. Animals were cared for in accordance with the guidelines established by the Animal Care and Use Committee of Kyushu University (Fukuoka, Japan).

Measurement of Locomotor Activity Rhythm—Mice were housed individually in breeding cages with food and water *ad libitum*. The cages were placed into an infrared ray area sensor, and locomotor activity was measured every 10 min. Locomotor activity was recorded under the light and dark cycles for 10 days and then continuously recorded under the constant dark condition for 10 days.

Anchorage-independent Cell Growth Assay—To evaluate the oncogenic transformation of cells, the ability of cells to grow in an anchorage-independent manner was assessed using the Quantitative 3D Cell Culture Colony Assay Kit (Nihon-ika Co. Ltd., Osaka, Japan). Cells were seeded in 10% FBS containing DMEM soft agar at a density of 1×10^4 cells. The viability of cells in agar was determined by tetrazolium chloride on day 7 after seeding.

Construction of Vectors—Retroviral plasmid vectors expressing H-ras^{V12} (Addgene plasmid#9051) and SV40LT (Addgene plasmid#13970) were transfected into G3T-hi packaging cells. All of the infected cells were cultured in medium containing the appropriate antibiotics. The mouse *Atf4* promoter region spanning bp −346 to +170 (these numbers represent the distance in base pairs from the putative transcription start site, +1) was amplified by PCR, and the product was ligated into the pGL3-Basic luciferase reporter vector (Promega). The E-box of the *Atf4* promoter was mutated at −83 to −78 (CACGTG to GAGTCT) using a QuikChange site-directed mutagenesis kit (Stratagene, La Jolla, CA). Expression vectors for mouse *Per2*, *Cry1*, *Bmal1*, *Clock*, and *ATF4* were also constructed using complementary DNAs (cDNAs) obtained by RT-PCR derived from mouse hepatic RNA. Coding regions were ligated into the pcDNA3.1 vectors (Invitrogen).

Histochemical Analysis—Cells were fixed with 4% paraformaldehyde/PBS for 10 min. Senescence-associated β-galactosidase (β-gal)-positive cells were detected using a senescence detection kit (BioVision, Inc. Palo Alto, CA). The percentage of β-gal-positive cells was determined by counting the number of positive cells in 3 randomly chosen fields at ×400 magnification.

Small Interfering RNA—Oncogene-transformed cells were transfected with siRNA against ATF4 (Santa Cruz Biotechnology, Inc. Dallas, TX). This siRNA is designed to prevent the expression of mouse ATF4 (15). Oncogene-introduced cells were transfected with the same amount of scrambled siRNA as the control and were then used in experiments 48 h after siRNA transfection.

RT-PCR Analysis—To quantify the mRNA levels of cellular senescence factors, cDNA was synthesized by reverse transcription using the ReverTra Ace quantitative real-time PCR kit (Toyobo, Osaka, Japan). Diluted cDNA samples were analyzed by PCR using the THUNDERBIRDSYBR qPCR Mix (Toyobo) and 7500 RT-PCR system (Applied Biosystems, Framingham, MA). To confirm the expression of H-ras^{V12} and SV40LT, diluted cDNA samples were also subjected to PCR as described above, and PCR products were run on agarose gel after staining with ethidium bromide. PCR primer sequences are described in Table 1.

Western Blotting—Nuclear or cytoplasmic proteins prepared from cells were separated on SDS-polyacrylamide gels and transferred to polyvinylidene difluoride membranes. The membranes were reacted with antibodies against activating transcription factor 4 (ATF4; sc-200, Santa Cruz Biotechnology), p16INK4a (sc-1207), p19ARF (sc-22784), retinoblastoma protein (pRB; sc-69791), p53 (sc-6243), PER2 (sc-25368), BMAL1 (sc-48790) ACTIN (sc-1616), or anti-phospho-pRB-Thr826 (44–576; BIOSOURCE International, Camarillo, CA). Specific antigen-antibody complexes were visualized using horseradish peroxidase-conjugated secondary antibodies and Chemi-Lumi One (Nacalai Tesque) or ImmunoStar reagent (Wako Chemical Co. Ltd., Tokyo, Japan).

[3] The abbreviations used are: MEF, mouse embryonic fibroblast; ATF4, activating transcription factor 4.

TABLE 1
Primer sets for PCR analysis

Gene	Primers
H-ras^{V12}	Forward, 5′-GACGGAATATAAGCTGGTGGT-3′
	Reverse, 5′-GTCCTTCACCCGTTTGATCTG-3′
SV40LT	Forward, 5′-AAAGCTGCACTGCTATACAA-3′
	Reverse, 5′-AATTGTAGGCTATCAACCCG-3′
Mouse *p16Ink4a*	Forward, 5′-GAACTCTTTCGGTCGTACCC-3′
	Reverse, 5′-CAGTTCGAATCTGCACCGTAG-3′
Mouse *p19Arf*	Forward, 5′-CATGTTGTTGAGGCTAGAGAGG-3′
	Reverse, 5′-TGAGCAGAAGAGCTGCTACG-3′
Mouse *p21*	Forward, 5′-TCTAGGGTGGGTCCTTGGTG-3′
	Reverse, 5′-CAGCCATTGCTCAGTGTCCT-3′
Mouse *Bax*	Forward, 5′-CAGGAGCGTCCACCAAGAA-3′
	Reverse, 5′-AGTAGAAGAGGGCAACCACG-3′
Mouse *Atf4*	Forward, 5′-CGAATGGATGACCTGGAAAC-3′
	Reverse, 5′-GGCTGCAAGAATGTAAAGGG-3′
Mouse *Per2*	Forward, 5′-CACCCTGAAAAGAAAGTGCGA-3′
	Reverse, 5′-CAACGCCAAGGAGCTCAAGT-3′
Mouse *Cry1*	Forward, 5′-AAGTCATCGTGCGCATTTCA-3′
	Reverse, 5′-TCATCATGGTCGTCGGACAGA-3′
Mouse *Cry2*	Forward, 5′-GGATAAGCACTTGGAACGGAA-3′
	Reverse, 5′-ACAAGTCCCACAGGCGGT-3′
Mouse *Bmal1*	Forward, 5′-CCGATGACGAACTGAAACACCT-3′
	Reverse, 5′-TGCAGTGTCCGAGGAAGATAGC-3′
Mouse *Clock*	Forward, 5′-TCTCTTCCAAACCAGACGCC-3′
	Reverse, 5′-TGCGGCATACTGGATGGAAT-3′
Mouse *β-actin*	Forward, 5′-CACACCTTCTACAATGAGCTGC-3′
	Reverse, 5′-CATGATCTGGGTCATCTTTTCA-3′

Immunoprecipitation—Oncogene-introduced wild type, *Per2*$^{m/m}$, and *Bmal1*$^{-/-}$ cells were lysed in 25 mmol/liter Tris-HCl, pH 8.0, 137 mmol/liter NaCl, 2.7 mmol/liter KCl, and 1% Triton X-100 supplemented with protease inhibitor mixtures and were then subjected to immunoprecipitation with anti-SV40LT antibodies (sc-58665, Santa Cruz Biotechnology). The amounts of p53, pRB, and SV40LT in cell lysates, supernatants, and immune complexes were detected by Western blotting.

Luciferase Reporter Assay—MEFs prepared from the wild type were seeded at a density of 1×10^5 cells/well on 24-well culture plates. Cells were transfected 18 h later with 100 ng/well of reporter vectors and 1–2 μg/well (total) of expression vectors. The pRL-TK vector (0.5 ng/well; Promega) was also co-transfected as an internal control reporter. Cells were then harvested, and cell lysates were analyzed using a dual-luciferase reporter assay system (Promega). The ratio of firefly (expressed from the reporter construct) to Renilla (expressed from pRL-TK) luciferase activities in each sample served as a measure of normalized luciferase activity.

Statistical and Data Analyses—To assess the endogenous period of each animal, locomotor counts were analyzed using ClockLab software (Actimetrics, Evanston, IL). The values presented are expressed as the means ± S.E. The significance of differences among groups was analyzed by analysis of variance followed by Tukey-Kramer's post hoc tests. Equal variances were not formally tested. $p < 0.05$ was considered significant.

Results

Different Oncogenic Phenotypes of Per2$^{m/m}$ *and Bmal1*$^{-/-}$ *Cells*—Spontaneous locomotor activity, which is an accurate measure of circadian activity, was monitored in wild-type, *Per2*$^{m/m}$, and *Bmal1*$^{-/-}$ mice. Animals were initially maintained on a 12-h light/dark cycle (*LD*) for 10 days and were subsequently maintained under constant darkness (*DD*) (Fig. 1). The locomotor activity of wild-type mice increased during the dark phase, so that they entrained to the scheduled dark lighting cycle (Fig. 1*A*). Under constant darkness condition, wild-type mice also exhibited robust circadian rhythms of locomotor activity, and their free-running periods were 23.67 ± 0.34 h ($n = 4$, mean ± S.E.). In contrast, neither *Per2*$^{m/m}$ nor *Bmal1*$^{-/-}$ mice failed to show entrained rhythms of locomotor activity even under LD cycle condition (Fig. 1, *B* and *C*). Furthermore, a spectral analysis of locomotor activity did not detect periodicity in the circadian range for *Per2*$^{m/m}$ or *Bmal1*$^{-/-}$ mice, suggesting that the apparent circadian rhythms are similarly disrupted even though the negative or positive components of the circadian clock are deleted.

To compare the roles of *Per2*$^{m/m}$ and *Bmal1*$^{-/-}$ in oncogenic transformation, we prepared MEFs from wild-type, *Per2*$^{m/m}$, and *Bmal1*$^{-/-}$ mice and infected cells concomitantly with retrovirus vectors expressing H-ras^{V12} and SV40LT (Fig. 1*D*). The expression of mRNAs for these oncogenes was detected on day 3 after infection, and they were equally expressed in all types of cells (Fig. 1*E*). The concomitant introduction of H-ras^{V12} and SV40LT significantly enhanced the anchorage-independent growth of wild-type and *Per2*$^{m/m}$ cells ($p < 0.01$, respectively, Fig. 1*F*), whereas the introduction of these oncogenes failed to enhance the growth of *Bmal1*$^{-/-}$ cells. These findings suggested that the loss of *Bmal1* resulted in the phenotype resisting oncogene-induced malignant transformation.

We also tested the tumorigenicity of oncogene-introduced cells using an implant model in mice. Equal numbers of wild-type, *Per2*$^{m/m}$, or *Bmal1*$^{-/-}$ cells infected with the oncogenes (H-ras^{V12} and SV40LT) were inoculated into the flanks of NOD-SCID mice. Although mice inoculated with wild-type and *Per2*$^{m/m}$ cells infected with oncogenes showed the significant growth of tumor masses (Fig. 1*G*), the average tumor volume in mice inoculated with *Per2*$^{m/m}$ cells was significantly larger than that in mice inoculated with wild-type cells ($p < 0.05$ on days 17, 20, and 23, respectively). In contrast, mice inoculated with oncogene-introduced *Bmal1*$^{-/-}$ cells showed no palpable tumor masses throughout the experimental period. Taken together, these results indicated that a deficiency in PER2 tended to enhance tumorigenicity, whereas the loss of BMAL1 resulted in the phenotype resisting oncogene-induced malignant transformation.

Oncogene Introduction Induces Cellular Senescence of Bmal1$^{-/-}$ *Cells*—During oncogenic transformation, growth signals that override the normal cell-cycle mechanism are activated in cancer cells, resulting in abnormal proliferation. Failure of cells to override this mechanism often causes reversible cell-cycle arrest, apoptotic cell death, or cellular senescence (16). In contrast to reversible cell-cycle arrest, cellular senescence is defined by the irreversible loss of proliferative potential, acquisition of a characteristic morphology, and expression of specific biomarkers, such as β-gal (17, 18). On day 14 after the infection with retrovirus vectors expressing H-ras^{V12} and SV40LT, the number of β-gal-positive *Bmal1*$^{-/-}$ cells was significantly higher than those among wild-type and *Per2*$^{m/m}$ cells ($p < 0.01$, Fig. 2*A*).

The tumor suppressor gene *Cdkn2a* acts as a canonical inducer of cellular senescence (18, 19). *Cdkn2a* generates the different transcript variants, *p16Ink4a* and *p19Arf* (also known as *p14ARF* in humans), by using different first exons and alter-

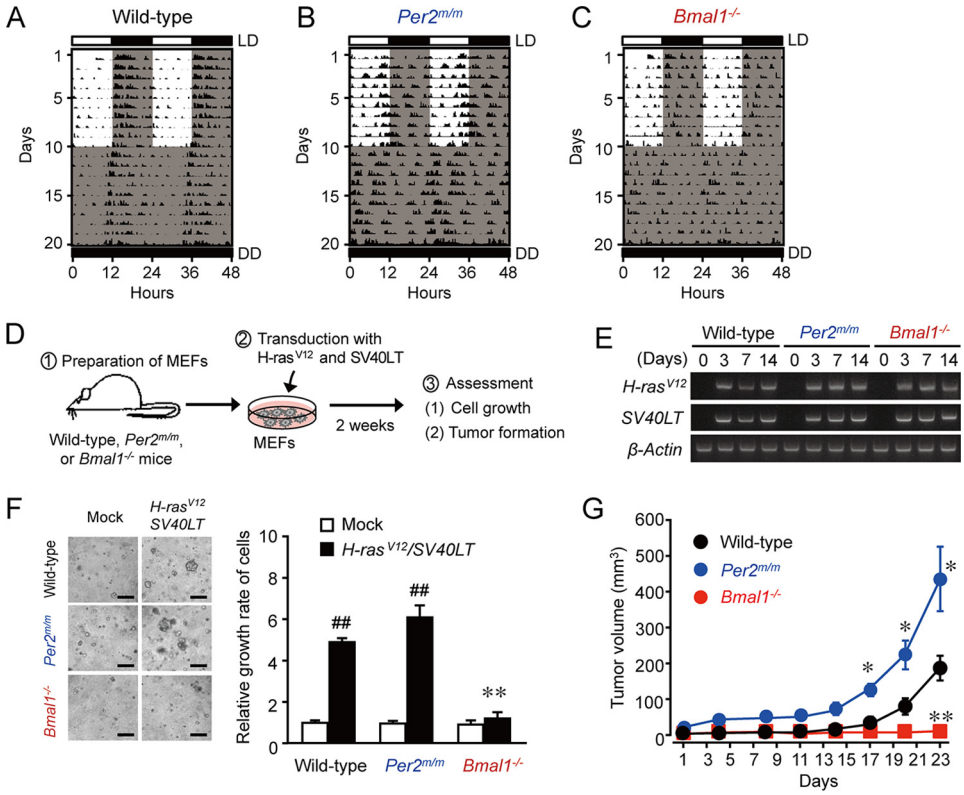

FIGURE 1. **Different oncogenic phenotypes of *Per2*$^{m/m}$ and *Bmal1*$^{-/-}$ cells after introduction of H-ras^{V12} and SV40LT.** *A–C*, representative locomotor activity records of wild-type (*A*), *Per2*$^{m/m}$ (*B*), or *Bmal1*$^{-/-}$ (*C*) mice. Light regime: 10 days in a 12-h light and 12-h dark cycle followed by 10 days in a constant dark cycle. *D*, schematic experimental procedure for evaluating the oncogenesis of clock gene-deficient cells. MEFs were prepared from wild-type, *Per2*$^{m/m}$, or *Bmal1*$^{-/-}$ mice. Cells were infected with retroviral vectors expressing H-ras^{V12} and SV40LT. *E*, the time course of mRNA expressions of *H-ras*^{V12} and *SV40LT* in wild-type, *Per2*$^{m/m}$, or *Bmal1*$^{-/-}$ cells after infection with retrovirus vectors expressing oncogenes. *F*, anchorage-independent growth of wild-type, *Per2*$^{m/m}$, and *Bmal1*$^{-/-}$ cells after the concomitant introduction of H-ras^{V12} and SV40LT. Cells infected with oncogenes were subjected to a soft-agar colony assay, and their colony formation and viability were assessed 14 days after seeding. Control cells were infected with mock vectors. The *left panels* show representative microscopic photographs of colony formation in each type of cells. The *scale bars* indicate 100 μm. The *right panel* shows viability of cells. Values are shown as means ± S.E. (n = 3–6). Mean values of mock-transfected wild-type cells were set at 1.0. ##, $p < 0.01$ significantly different from the mock-transfected group. **, $p < 0.01$ significantly different from oncogene-transfected wild-type and *Per2*$^{m/m}$ cells. *G*, tumor formation by oncogene-introduced wild-type, *Per2*$^{m/m}$, or *Bmal1*$^{-/-}$ cells. Equal numbers of cells (5×10^6 cells) were implanted into the dorsal air sacs of NOD/SCID mice. Values are the means ± S.E. (n = 4). **, $p < 0.01$; *, $p < 0.05$ significantly different from the other groups at the corresponding time points.

nate polyadenylation sites (20, 21). The *p16Ink4a* variants encode structurally related protein isoforms that inhibit CDK4 kinase (19). The CDK4 inhibitor prevents the phosphorylation of pRB by disrupting the activity of the CDK4-cyclin D complex. On the other hand, p19ARF stabilizes p53 by sequestering MDM2 (22). The mRNA levels of *p16Ink4a* and *p19Arf* were significantly increased in oncogene-introduced *Bmal1*$^{-/-}$ cells ($p < 0.01$, respectively; Fig. 2*B*), whereas the mRNA levels of both transcript variants of *Cdkn2a* in wild-type and *Per2*$^{m/m}$ cells were slightly but significantly decreased by the introduction of oncogenes. Consistent with these results, marked increases in the protein levels of p16INK4a and p19ARF were also detected in oncogene-introduced *Bmal1*$^{-/-}$ cells (Fig. 2*C*), whereas those protein levels were decreased in oncogene-introduced wild-type and *Per2*$^{m/m}$ cells. The induction of cellular senescence factors in oncogene-introduced *Bmal1*$^{-/-}$ cells was accompanied by the suppressed phosphorylation of pRB as well as increases in the protein levels of p53 (Fig. 2*C*). These results suggested that oncogene-introduced *Bmal1*$^{-/-}$ cells failed to override the normal cell-cycle mechanism, resulting in cellular senescence.

SV40LT-transduced cells are considered to be insensitive to growth arrest by p16INK4a and p19ARF, because SV40LT inactivates p53 by protein-protein interaction (23). The results of an immunoprecipitation analysis revealed that the most amounts of p53 protein in oncogene-introduced wild-type and *Per2*$^{m/m}$ cells were precipitated together with SV40LT (Fig. 3*A*). On the other hand, large amounts of p53 protein in *Bmal1*$^{-/-}$ cells was unable to be precipitated together with SV40LT, suggesting that extensive expression of p53 in oncogene-introduced *Bmal1*$^{-/-}$ cells overrides the binding capacity of SV40LT. In fact, the expression of the p53 target genes, *p21* and *Bax*, was increased in oncogene-introduced *Bmal1*$^{-/-}$ cells (Fig. 3*B*).

The transforming activity of SV40LT has also been attributed to its perturbation of pRb (24). Although large amounts of pRb were precipitated together with SV40LT, the protein was also detected in the supernatant fractions of all cell types (Fig. 3*A*). These results indicated that the growth inhibitory function of pRb still remained in oncogene-introduced wild-type, *Per2*$^{m/m}$, and *Bmal1*$^{-/-}$ cells. The retroviral transfer of SV40LT into these cells appeared to partially suppress pRb function.

In an attempt to determine whether accumulation of p53 in oncogene-introduced *Bmal1*$^{-/-}$ cells contributes to the induction of cellular senescence, oncogene-introduced wild-type and

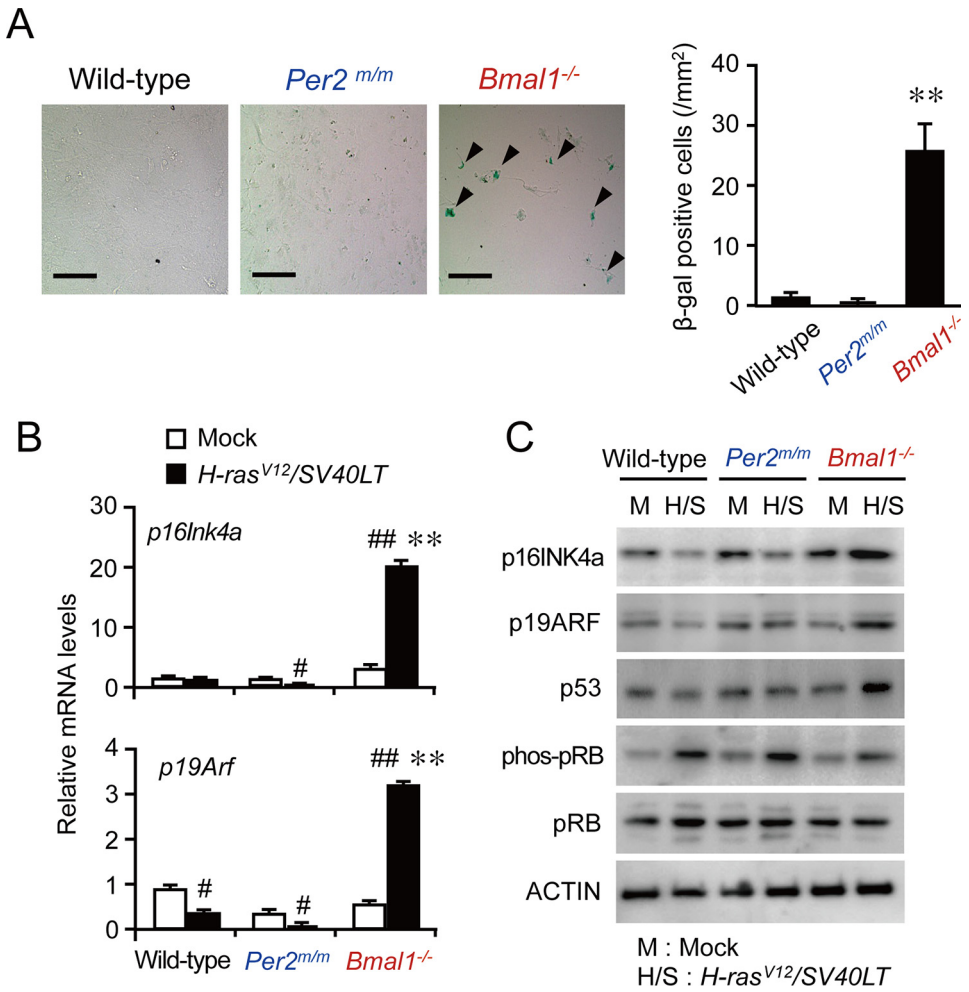

FIGURE 2. **Induction of cellular senescence in oncogene-introduced *Bmal1*$^{-/-}$ cells.** *A*, β-gal staining of wild-type, *Per2*$^{m/m}$, or *Bmal1*$^{-/-}$ cells infected with H-ras^{V12} and SV40LT. *Arrows* in the microscopic photograph indicate β-gal-positive cells. The *scale bars* indicate 50 μm. Values are the means ± S.E. ($n = 3$). **, $p < 0.01$ significantly different from other oncogene-introduced cells. *B*, the mRNA levels of *p16Ink4a* and *p19Arf* in wild-type, *Per2*$^{m/m}$, or *Bmal1*$^{-/-}$ cells infected with oncogenes. Values are the means ± S.E. ($n = 3$). ##, $p < 0.01$ significantly different from mock-transfected group. **, $p < 0.01$ significantly different from other oncogene-introduced cells. *C*, the protein abundance of p16INK4a, p19ARF, p53, phosphorylated pRB (*phos-pRB*), and pRB in wild-type, *Per2*$^{m/m}$, or *Bmal1*$^{-/-}$ cells infected with oncogenes.

Bmal1$^{-/-}$ cells were incubated in the presence and absence of the p53 inhibitor pifithrin-α. The treatment with 30 μM pifithrin-α had a negligible effect on the anchorage-independent growth of oncogene-introduced wild-type cells but significantly enhanced the growth of oncogene-introduced *Bmal1*$^{-/-}$ cells ($p < 0.01$, Fig. 3*C*). Extensive expression of p53 in oncogene-introduced *Bmal1*$^{-/-}$ cells appeared to override the binding capacity of SV40LT and allowed the induction of cellular senescence.

ATF4 Determines the Oncogenic Phenotypes of Per2$^{m/m}$ *and Bmal1*$^{-/-}$ *Cells*—A member of the cAMP-binding protein family, ATF4, promotes oncogene-induced transformation by suppressing the expression of p16INK4a and p19ARF (15). The protein levels of ATF4 were substantially increased in oncogene-introduced wild-type and *Per2*$^{m/m}$ cells but not in *Bmal1*$^{-/-}$ cells (Fig. 4*A*). The excessive expression of ATF4 in oncogene-introduced *Per2*$^{m/m}$ cells was repressed by the transfection of functional "native" Per2-expressing vectors (Fig. 4*B*), whereas the transfection of oncogene-introduced *Bmal1*$^{-/-}$ cells with Bmal1-expressing vectors caused an increase in ATF4 levels (Fig. 4*C*). The modulation of ATF4 protein levels by PER2 and BMAL1 occurred at the transcriptional level because the mRNA levels of *Atf4* were also down- and up-regulated by PER2 and BMAL1, respectively (Fig. 4, *B* and *C*).

The transfection of oncogenic wild-type and *Per2*$^{m/m}$ cells with siRNA against *Atf4* decreased ATF4 protein levels as well as the phosphorylation of pRB (Fig. 4*D*). The down-regulation of ATF4 in both types of cells increased the protein levels of p16INK4a and p19ARF, but the effect was greater on p16INK4a than on p19ARF (Fig. 4*D*). Furthermore, anchorage-independent growth of oncogene-introduced wild-type and *Per2*$^{m/m}$ cells was significantly suppressed by down-regulation of ATF4 ($p < 0.01$ for wild-type cells; $p < 0.05$ for *Per2*$^{m/m}$ cells, Fig. 4*E*). On the other hand, the transfection of oncogene-introduced *Bmal1*$^{-/-}$ cells with ATF4-expressing vectors decreased the protein levels of p16INK4a and p19ARF (Fig. 4*F*), whereas these protein levels in oncogene-introduced wild-type cells were not markedly affected by the transfection of ATF4-expressing vectors. The overexpression of ATF4 in *Bmal1*$^{-/-}$ cells also significantly enhanced their anchorage-independent growth ability ($p < 0.01$, Fig. 4*G*). These results

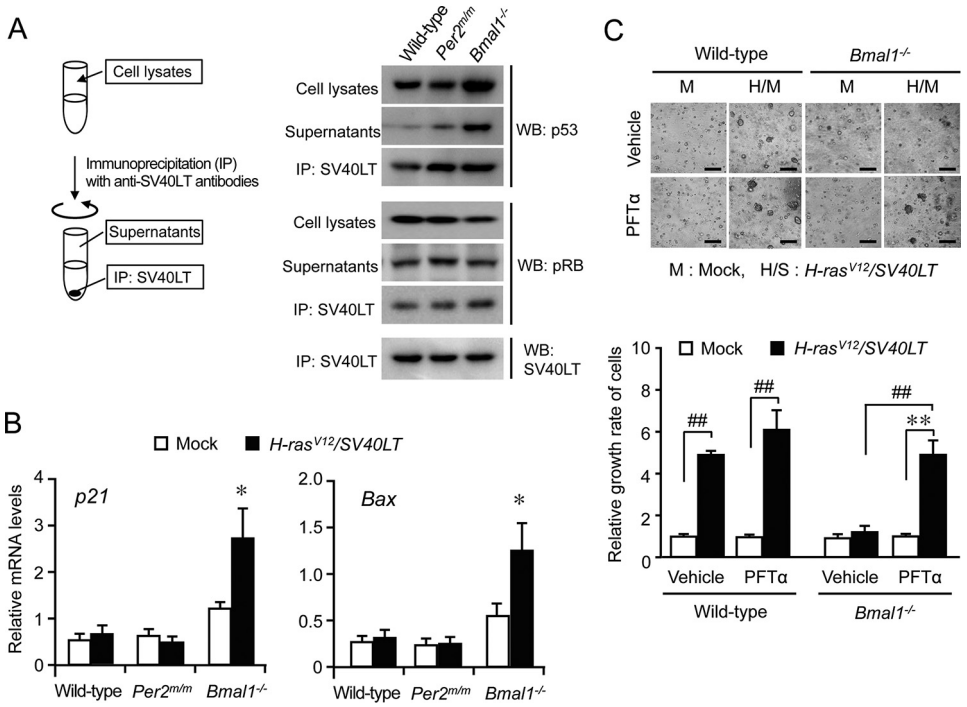

FIGURE 3. **The overexpression of p53 in oncogene-introduced *Bmal1*$^{-/-}$ cells overrides the binding capacity of SV40LT.** *A*, the oncogene-introduced wild-type, *Per2*$^{m/m}$, or *Bmal1*$^{-/-}$ cells were lysed and were then subjected to immunoprecipitation with anti-SV40LT antibodies. The amounts of p53, pRb, and SV40LT in cell lysates, supernatants, and immune complexes were detected by Western blotting (*WB*). *B*, the mRNA levels of p53 target genes, *p21* and *Bax*, in wild-type, *Per2*$^{m/m}$, or *Bmal1*$^{-/-}$ cells infected with oncogenes. Values are the means ± S.E. ($n = 3$). *, $p < 0.05$ significantly different from other oncogene-introduced cells. *C*, influence of p53 inhibitor Pifithrin-α (*PFTα*) on the anchorage-independent growth of wild-type and *Bmal1*$^{-/-}$ cells after the concomitant introduction of H-ras^{V12} and SV40LT. Cells infected with oncogenes were subjected to a soft agar colony assay in the presence or absence of 30 μM pifithrin-α. The colony formation of cells and their viability were assessed 14 days after seeding. Control cells were infected with mock vectors. The *upper panels* show representative microscopic photographs of colony formation in each type of cells. The *scale bars* indicate 100 μm. The *lower panel* shows viability of cells. Values are shown as the means ± S.E. ($n = 4$). Mean values of mock-transfected wild-type cells were set at 1.0. ##, $p < 0.01$; **, $p < 0.01$ significantly different between the two groups.

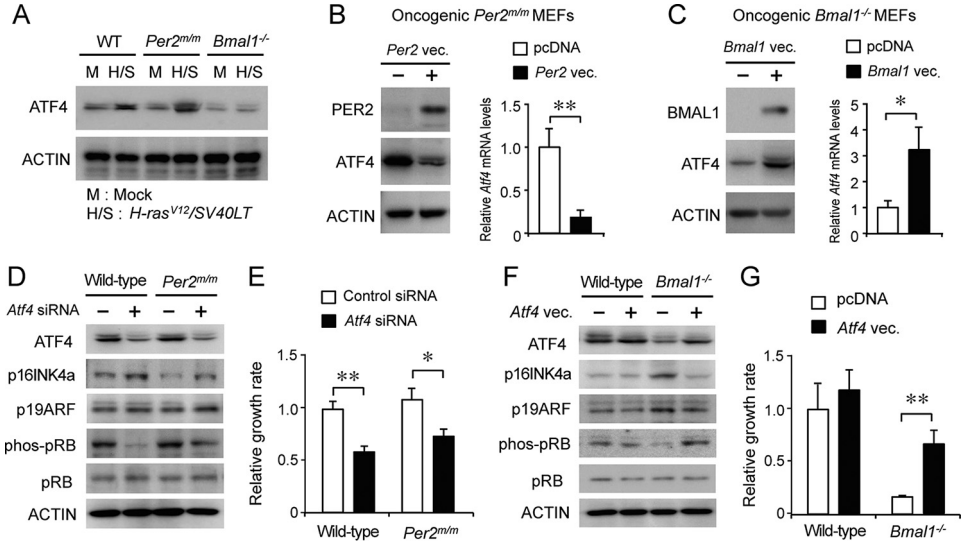

FIGURE 4. **Role of ATF4 in the oncogene-induced transformation of *Per2 or Bmal1*-defective cells.** *A*, the protein levels of ATF4 in wild-type, *Per2*$^{m/m}$, or *Bmal1*$^{-/-}$ cells infected with H-ras^{V12} and SV40LT. *B*, the overexpression of PER2 in oncogene-introduced *Per2*$^{m/m}$ cells suppresses the expression of ATF4. *C*, the overexpression of BMAL1 in oncogene-introduced *Bmal1*$^{-/-}$ cells enhances the expression of ATF4. For *panels B* and *C*, the mean value of empty vectors (*pcDNA*)-transfected cells were set at 1.0. *D*, influence of siRNA-induced down-regulation of *Atf4* on the protein abundance of p16INK4a, p19ARF, p53, phosphorylated pRB (*phos-pRB*), and pRB in wild-type or *Per2*$^{m/m}$ cells. *E*, down-regulation of ATF4 in oncogene-introduced wild-type or *Per2*$^{m/m}$ cells by siRNA attenuated anchorage-independent growth ability. *F*, the protein abundance of p16INK4a, p19ARF, p53, phosphorylated pRB (*phos-pRB*), and pRB in oncogenic wild-type or *Bmal1*$^{-/-}$ cells transfected with *Atf4*-expressing vectors. *G*, overexpression of ATF4 in oncogene-introduced *Bmal1*$^{-/-}$ cells enhanced the anchorage-independent growth ability. For panels *B*, *C*, *E*, and *G*, values are shown as the mean ± S.E. ($n = 4$). **, $p < 0.01$, *, $p < 0.05$ significantly different between the two groups.

suggested that the tumorigenicity of clock gene-defective cells was dependent on the responsiveness of ATF4 to the introduction of oncogenes.

Different Oncogenic Phenotypes of Cry1/2$^{-/-}$ *and Clk/Clk Cells*—Next, we also investigated the tumorigenicity of other clock gene-defective cells. CRY proteins act as negative tran-

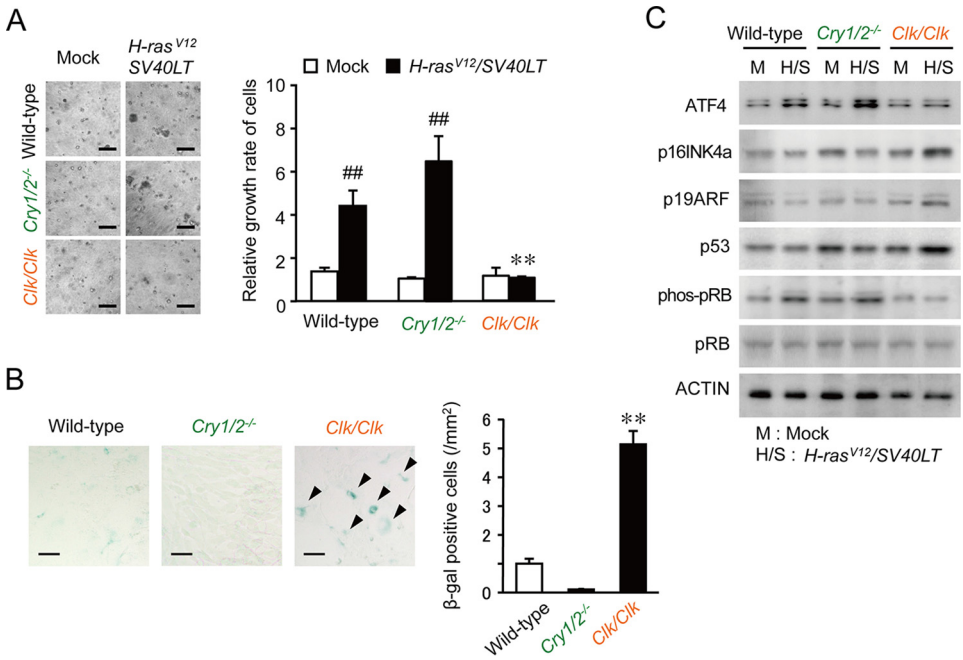

FIGURE 5. **Different responses of *Cry1/2*- or *Clock*-defective cells to oncogene-induced transformation.** *A*, anchorage-independent growth of wild-type, *Cry1/2*$^{-/-}$, or *Clk/Clk* cells after the concomitant introduction of H-ras^{V12} and SV40LT. Cells infected with oncogenes were subjected to a soft-agar colony assay, and their colony formation and viability were assessed 14 days after seeding. Control cells were infected with mock vectors. The *left panels* show representative microscopic photographs of colony formation in each type of cells. The *scale bars* indicate 100 μm. The *right panel* shows viability of cells. Values are shown as the means ± S.E. ($n = 4$). Mean values of mock-transfected wild-type cells were set at 1.0. ##, $p < 0.01$ significantly different from the mock-transfected group. **, $p < 0.01$ significantly different from oncogene-transfected wild-type and *Cry1/2*$^{-/-}$ cells. *B*, β-gal staining of wild-type, *Cry1/2*$^{-/-}$, or *Clk/Clk* cells infected with oncogenes. *Arrows* in the microscopic photograph indicate β-gal-positive cells. The *scale bars* indicate 50 μm. Values are the means ± S.E. ($n = 3$). **, $p < 0.01$ significantly different from other oncogene-introduced cells. *C*, the protein abundance of p16INK4a, p19ARF, p53, phosphorylated pRB (*phos-pRB*), and pRB in wild-type, *Cry1/2*$^{-/-}$, or *Clk/Clk* cells infected with oncogenes.

scriptional regulators of circadian feedback loops. *Cry*-null mice, defective in both *Cry1* and *Cry2* (*Cry1/2*$^{-/-}$), accordingly show arrhythmic behavior, physiology, and metabolism (25). In addition, the CLOCK protein heterodimerizes with BMAL1 and acts as a positive transcriptional regulator in the circadian clock machinery. *Clk*/*Clk* mice also exhibit abnormal rhythms in physiology and behavior (26, 27). The concomitant introduction of H-ras^{V12} and SV40LT significantly enhanced the anchorage-independent growth of *Cry1/2*$^{-/-}$ cells ($p < 0.01$) but did not promote the growth of *Clk*/*Clk* cells (Fig. 5*A*). In contrast, on day 14 after the infection with retrovirus vectors expressing oncogenes, the number of β-gal-positive *Clk*/*Clk* cells was significantly higher than those among wild-type and *Cry1/2*$^{-/-}$ cells ($p < 0.01$ respectively; Fig. 5*B*). The retroviral transfer of H-ras^{V12} and SV40LT into *Clk*/*Clk* cells had a negligible effect on ATF4 protein levels, whereas oncogene introduction enhanced the expression of p16INK4a, p19AFR, and p53 (Fig. 5*C*). These results also supported negative and positive regulators of circadian clock playing different roles in neoplastic transformation induced by the introduction of H-ras^{V12} and SV40LT.

Transcriptional Regulation of Atf4 by Products of Clock Genes—In the final set of experiments, we investigated the mechanisms by which circadian clock genes modulate ATF4 expression during oncogenic transformation. The mRNAs for *Per2*, *Cry1*, *Cry2*, *Bmal1*, and *Clock* were detected in normal wild-type cells (day 0). Their mRNA levels were elevated after the concomitant introduction of H-ras^{V12} and SV40LT; however, the time courses of mRNA elevations in oncogene-introduced cells were similar to those observed in cells that were infected with mock vectors (Fig. 6*A*). In contrast, the introduction of H-ras^{V12} and SV40LT into wild-type cells significantly increased the mRNA levels of *Atf4* ($p < 0.05$).

The products of *Bmal1* and *Clock* have been shown to positively regulate the expression of their target genes through an E-box (CACGTG) element (1, 2). BMAL1/CLOCK-mediated transactivation is repressed by PERs or CRYs. An E-box motif has been detected upstream of the *Atf4* gene in mice and all mammals examined, including rats, chimpanzees, and humans (28, 29). The activity of the luciferase reporter of the mouse *Atf4* promoter region containing the E-box (native *Atf4*::Luc) was enhanced when it was transfected into oncogene-transformed wild-type cells (Fig. 6*B*). The enhanced reporter activity of native *Atf4*::Luc was repressed by the co-transfection with *Per2*- or *Cry1*-expressing vectors. In contrast, the co-transfection with *Bmal1*- or *Clock*-expressing vectors further enhanced the reporter activity of native *Atf4*::Luc in oncogene-transformed wild-type cells. Although the reporter activity of E-box-mutated *Atf4* luciferase constructs (E-box mut. *Atf4*::Luc) was also enhanced in oncogene-transformed wild-type cells (Fig. 6*B*), enhanced reporter activity was not further modulated by the co-transfection with *Per2*- and *Bmal1*-expressing vectors. These results indicated that the oncogene-induced transformation of cells resulted in elevations in ATF4 levels without affecting clock gene expression, whereas components of the circadian clock appeared to influence the expression of *Atf4* in oncogenic cells through E-box elements.

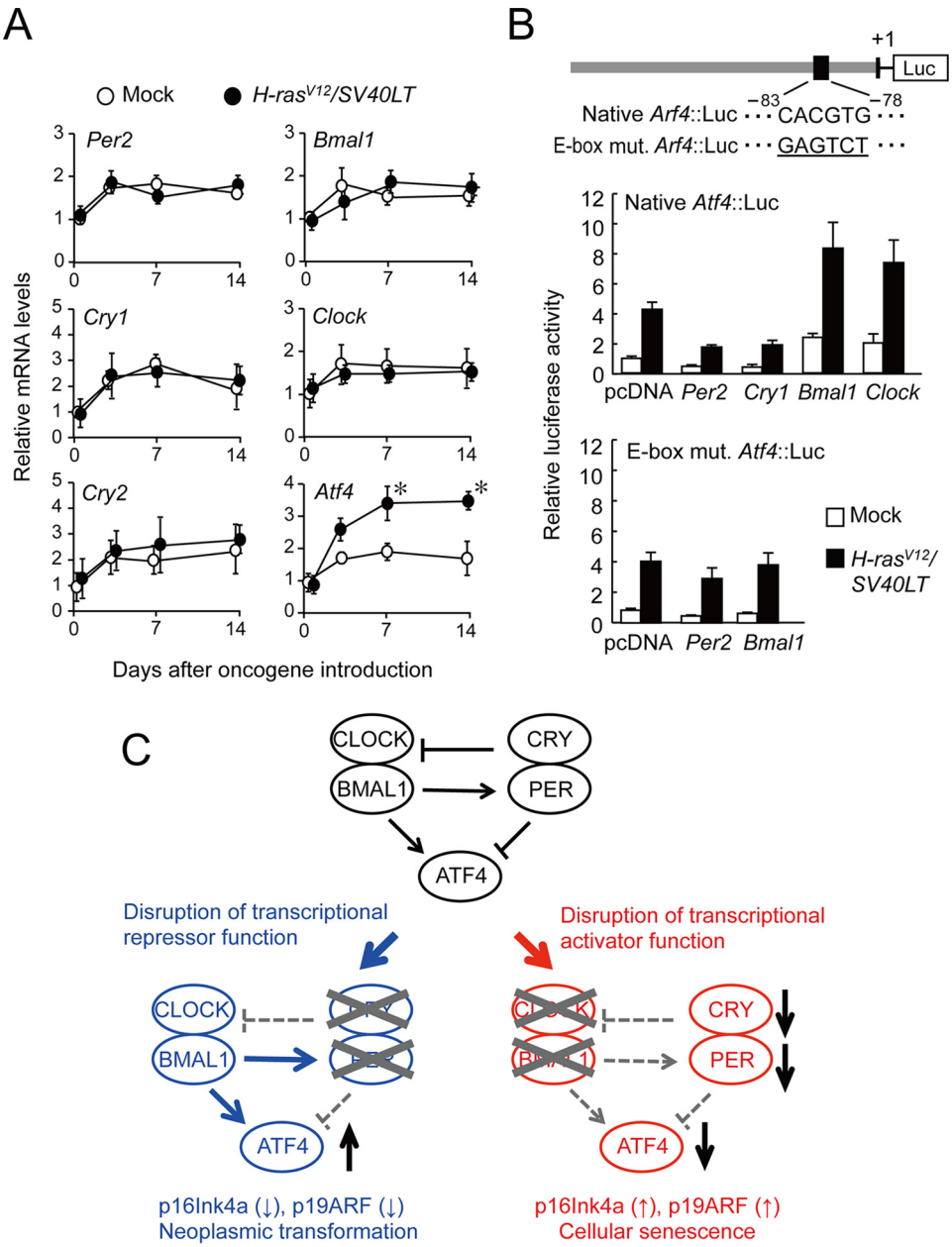

FIGURE 6. **Transcriptional regulation of *Atf4* gene by clock gene products.** *A*, the time course of mRNA expressions of *Per2*, *Cry1*, *Cry2*, *Bmal1*, *Clock*, and *Atf4* in wild-type cells after infection with retrovirus vectors expressing H-ras^{V12} and SV40LT. Mean values of mock-transfected cells on day 0 are set at 1.0. Values are shown as the mean ± S.E. ($n = 3$). *, $p < 0.05$ as compared with mock-transfected group at corresponding time points. *B*, luciferase reporter assay of the mouse *Atf4* promoter in oncogene introduced wild-type cells. The *upper panel* shows a schematic representation of the mouse *Atf4* promoter. *Numbers below the boxes* are nucleotide residues positioned relative to transcription start site (+1). *Underlined nucleotide residues* indicate a mutated sequence of E-box. Wild-type MEFs and oncogene-introduced wild-type MEFs were transfected with 0.1 μg of each native *Atf4*::Luc or E-box mutated *Atf4*::Luc (*E-box mut. Atf4::Luc*). Cells transfected with reporter constructs were also co-transfected with expressing constructs for *Per2*, *Cry1*, *Bmal1*, or *Clock*. Values are expressed as relative ratio to the *Atf4*::Luc activity of wild-type MEFs in the absence of expressing vectors (set at 1.0). All values are shown as the means ± S.E. ($n = 4$). *C*, possible mechanisms for the promotion of oncogenicity by disruptions in the molecular circadian clock. When the circadian clock is disrupted due a dysfunction in the transcriptional repressor PER or CRY, ATF4 is markedly expressed by oncogenic stimuli, and cells easily undergo malignant transformation. In contrast, when the circadian clock is disrupted due to a dysfunction in the transcriptional activator CLOCK or BMAL1, ATF4 is hardly expressed by oncogenic stimuli, and p16INK4a and p19ARF induce cellular senescence.

Discussion

The results of the present study suggest the opposite roles for the negative and positive components of the circadian clock in oncogene-induced transformation. As shown in Fig. 6*C*, when the circadian rhythms are disrupted due to a dysfunction in the transcriptional repressor PER or CRY, the expression of ATF4 is facilitated by oncogenic stimuli, and cells override normal cell cycle mechanism, and easily undergo malignant transformation. By contrast, when the circadian rhythms are disrupted due to a dysfunction in the transcriptional activator BMAL1 or CLOCK, ATF4 is unresponsive to oncogenic stimuli, and elevations in the expression of p16INK4a and p19ARF causes cellular senescence. Consequently, oncogene-introduced *Bmal1*- or *Clock*-defective cells fail to override the normal cell-cycle mechanism.

ATF4 is ubiquitously expressed throughout the body and is induced in response to various stress signals, including anoxia, hypoxia, endoplasmic reticulum stress, amino acid deprivation, and oxidative stress (29). The stress-induced expression of ATF4 causes adaptive responses in cells through regulating the expression of target genes involved in amino acid synthesis, differentiation, metastasis, angiogenesis, and drug resistance (30). The expression of ATF4 is also under the control of the circadian clock (28). BMAL1:CLOCK heterodimers activate the transcription of *Atf4* through E-box enhancer elements, but this transactivation is repressed by PER and CRY. The reporter activity of native *Atf4*::Luc in oncogene-introduced cells was further enhanced by *Bmal1*- and *Clock*-expressing vectors. Therefore, the expression of ATF4 appeared to be diminished in *Bmal1*- or *Clock*-defective cells even when those cells were introduced with oncogenes. On the other hand, in the absence of negative circadian regulator PER and CRY, ATF4 seemed to be markedly expressed in response to oncogenic stimuli. Excessive expression of ATF4 is often observed in malignant tumors in humans and rodents (30). The highly expressed ATF4 is thought to facilitate tumor progression, because transcription of genes involved in tumor cell proliferation is modulated by ATF4 (31).

We previously reported that ATF4 promotes the oncogene-induced neoplastic transformation of MEFs by suppressing the expression of p16INK4a and p19ARF (15). The introduction of H-ras^{V12} and SV40LT into wild-type MEFs induces the expression of the *Atf4* gene along with that of p16INK4a and p19ARF. Elevations in ATF4 protein levels suppress the expression of these cellular senescence factors and drive oncogenic transformation. Therefore, elevated levels of ATF4 in oncogene-introduced wild-type and *Per2*$^{m/m}$ cells may be sufficient to suppress the expression of p16INK4a and p19ARF. Conversely, low levels of ATF4 in *Bmal1*$^{-/-}$ cells appear to allow the constitutive expression of these cellular senescence factors.

In this study we used retrovirus vectors expressing SV40LT as a transforming agent together with H-ras^{V12}. Because SV40LT inactivates p53 by protein-protein interactions and also perturbs the function of pRb (23, 24), SV40LT-transduced cells are considered to be insensitive to growth arrest by p16INK4a and p19ARF. Inactivation of the growth-suppressive properties of p53 and pRb was previously shown to be essential for the immortalization of MEFs by SV40LT. The concomitant introduction of H-ras^{V12} and SV40LT induced elevations in p53 protein levels in *Bmal1*$^{-/-}$ cells. p53 protein levels were markedly larger in oncogene-introduced *Bmal1*$^{-/-}$ cells than in wild-type and *Per2*$^{m/m}$ cells. Significant amounts of p53 protein in *Bmal1*$^{-/-}$ cells was unable to be precipitated together with SV40LT. In addition, there were no significant mutations in the p53 gene or p16Ink4a gene among wild-type, *Per2*$^{m/m}$, and *Bmal1*$^{-/-}$ cells (supplemental Fig. S1). Extensive expression of p53 in oncogene-introduced *Bmal1*$^{-/-}$ cells overrode the binding capacity of SV40LT. Therefore, untrapped/free p53 protein may allow the induction of cellular senescence. On the other hand, in wild-type, *Per2*$^{m/m}$, and *Bmal1*$^{-/-}$ cells, a large amount of pRb was unable to be precipitated together with SV40LT. The growth inhibitory function of pRb still remained in all cell types after the infection of oncogenes. The function of the remained pRb may be modulated by p16INK4a.

Although genetic ablation of either negative or positive components of the circadian clock leads to disrupted rhythm in physiological functions, our findings define the different contributions of each component of the circadian clock to neoplastic transformation. The fundamental mechanism of the mammalian circadian clock is conserved beyond the species (32). Similar mechanism may function in human cells during oncogenic transformation associated with the disruption of circadian clock machinery.

Author Contributions—C. K., S. K., and S. O. designed the study and wrote the paper. C. K. and S. K. performed and analyzed the experiments shown in Figs. 1–6. S. Shiromizu, N. Matsunaga, S. Shimba S., and S. Shibata provided technical assistance and contributed to the preparation of the figures. All authors reviewed the results and approved the final version of the manuscript.

Acknowledgments—Cry-null MEFs were kindly provided by Dr. Ueda (The University of Tokyo). We thank the Research Support Center, Graduate School of Medical Sciences, Kyushu University for technical support.

References

1. Dibner, C., Schibler, U., and Albrecht, U. (2010) The mammalian circadian timing system: organization and coordination of central and peripheral clocks. *Annu. Rev. Physiol.* **72,** 517–549
2. Partch, C. L., Green, C. B., and Takahashi, J. S. (2014) Molecular architecture of the mammalian circadian clock. *Trends Cell Biol.* **24,** 90–99
3. Gachon, F., Olela, F. F., Schaad, O., Descombes, P., and Schibler, U. (2006) The circadian PAR-domain basic leucine zipper transcription factors DBP, TEF, and HLF modulate basal and inducible xenobiotic detoxification. *Cell Metab.* **4,** 25–36
4. Gréchez-Cassiau, A., Rayet, B., Guillaumond, F., Teboul, M., and Delaunay, F. (2008) The circadian clock component BMAL1 is a critical regulator of p21WAF1/CIP1 expression and hepatocyte proliferation. *J. Biol. Chem.* **283,** 4535–4542
5. Panda, S., Antoch, M. P., Miller, B. H., Su, A. I., Schook, A. B., Straume, M., Schultz, P. G., Kay, S. A., Takahashi, J. S., and Hogenesch, J. B. (2002) Coordinated transcription of key pathways in the mouse by the circadian clock. *Cell* **109,** 307–320
6. Masri, S., Kinouchi, K., and Sassone-Corsi, P. (2015) Circadian clocks, epigenetics, and cancer. *Curr. Opin. Oncol.* **27,** 50–56
7. Lahti, T. A., Partonen, T., Kyyrönen, P., Kauppinen, T., and Pukkala E. (2008) Night-time work predisposes to non-Hodgkin lymphoma. *Int. J. Cancer* **123,** 2148–2151
8. Kloog, I., Haim, A., Stevens, R. G., and Portnov, B. A. (2009) Global co-distribution of light at night (LAN) and cancers of prostate, colon, and lung in men. *Chronobiol. Int.* **26,** 108–125
9. Filipski, E., Innominato, P. F., Wu, M., Li, X. M., Iacobelli, S., Xian, L. J., and Lévi, F. (2005) Effects of light and food schedules on liver and tumor molecular clocks in mice. *J. Natl. Cancer Inst.* **97,** 507–517
10. Lee, S., Donehower, L. A., Herron, A. J., Moore, D. D., and Fu, L. (2010) Disrupting circadian homeostasis of sympathetic signaling promotes tumor development in mice. *PLoS ONE* **5,** e10995
11. Fu, L., Pelicano, H., Liu, J., Huang, P., and Lee, C. (2002) The circadian gene Period2 plays an important role in tumor suppression and DNA damage response *in vivo*. *Cell* **111,** 41–50
12. Jozefczuk, J., Drews, K., and Adjaye, J. (2012) Preparation of mouse embryonic fibroblast cells suitable for culturing human embryonic and induced pluripotent stem cells. *J. Vis. Exp.* **64,** 3854
13. Ukai-Tadenuma, M., Yamada, R. G., Xu, H., Ripperger, J. A., Liu, A. C., and Ueda, H. R. (2011) Delay in feedback repression by cryptochrome 1 is

required for circadian clock function. *Cell* **144,** 268–281
14. Kakumoto, K., Sasai, K., Sukezane, T., Oneyama, C., Ishimaru, S., Shibutani, K., Mizushima, H., Mekada, E., Hanafusa, H., and Akagi, T. (2006) FRA1 is a determinant for the difference in RAS-induced transformation between human and rat fibroblasts. *Proc. Natl. Acad. Sci. U.S.A.* **103,** 5490–5495
15. Horiguchi, M., Koyanagi, S., Okamoto, A., Suzuki, S. O., Matsunaga, N., and Ohdo, S. (2012) Stress-regulated transcription factor ATF4 promotes neoplastic transformation by suppressing expression of the INK4a/ARF cell senescence factors. *Cancer Res.* **72,** 395–401
16. Hanahan, D., and Weinberg, R. A. (2011) Hallmarks of cancer: the next generation. *Cell* **144,** 646–674
17. Collado, M., Gil, J., Efeyan, A., Guerra, C., Schuhmacher, A. J., Barradas, M., Benguría, A., Zaballos, A., Flores, J. M., Barbacid, M., Beach, D., and Serrano, M. (2005) Tumour biology: senescence in premalignant tumours. *Nature* **436,** 642
18. Collado, M., and Serrano, M. (2010) Senescence in tumours: evidence from mice and humans. *Nat. Rev. Cancer* **10,** 51–57
19. Kim, W. Y., and Sharpless, N. E. (2006) The regulation of INK4/ARF in cancer and aging. *Cell* **127,** 265–275
20. Kamijo, T., Zindy, F., Roussel, M. F., Quelle, D. E., Downing, J. R., Ashmun, R. A., Grosveld, G., and Sherr, C. J. (1997) Tumor suppression at the mouse INK4a locus mediated by the alternative reading frame product p19ARF. *Cell* **91,** 649–659
21. Sharpless, N. E. (2005) INK4a/ARF: a multifunctional tumor suppressor locus. *Mutat. Res.* **576,** 22–38
22. Sherr, C. J. (2006) Divorcing ARF and p53: an unsettled case. *Nat. Rev. Cancer* **6,** 663–673
23. Zhu, J. Y., Abate, M., Rice, P. W., and Cole, C. N. (1991) The ability of simian virus 40 large T antigen to immortalize primary mouse embryo fibroblasts cosegregates with its ability to bind to p53. *J. Virol.* **65,** 6872–6880
24. Zalvide, J., and DeCaprio, J. A. (1995) Role of pRb-related proteins in simian virus 40 large-T-antigen-mediated transformation. *Mol. Cell Biol.* **15,** 5800–5810
25. van der Horst, G. T., Muijtjens, M., Kobayashi, K., Takano, R., Kanno, S., Takao, M., de Wit, J., Verkerk, A., Eker, A. P., van Leenen, D., Buijs, R., Bootsma, D., Hoeijmakers, J. H., and Yasui, A. (1999) Mammalian Cry1 and Cry2 are essential for maintenance of circadian rhythms. *Nature* **398,** 627–630
26. Vitaterna, M. H., King, D. P., Chang, A. M., Kornhauser, J. M., Lowrey, P. L., McDonald, J. D., Dove, W. F., Pinto, L. H., Turek, F. W., and Takahashi, J. S. (1994) Mutagenesis and mapping of a mouse gene, Clock, essential for circadian behavior. *Science* **264,** 719–725
27. Turek, F. W., Joshu, C., Kohsaka, A., Lin, E., Ivanova, G., McDearmon, E., Laposky, A., Losee-Olson, S., Easton, A., Jensen, D. R., Eckel, R. H., Takahashi, J. S., and Bass, J. (2005) Obesity and metabolic syndrome in circadian Clock mutant mice. *Science* **308,** 1043–1045
28. Koyanagi, S., Hamdan, A. M., Horiguchi, M., Kusunose, N., Okamoto, A., Matsunaga, N., and Ohdo, S. (2011) cAMP-response element (CRE)-mediated transcription by activating transcription factor-4 (ATF4) is essential for circadian expression of the Period2 gene. *J. Biol. Chem.* **286,** 32416–32423
29. Ameri, K., and Harris, A. L. (2008) Activating transcription factor 4. *Int. J. Biochem. Cell Biol.* **40,** 14–21
30. Ye, J., Kumanova, M., Hart, L. S., Sloane, K., Zhang, H., De Panis, D. N., Bobrovnikova-Marjon, E., Diehl, J. A., Ron, D., and Koumenis, C. (2010) The GCN2-ATF4 pathwayis critical for tumourcell survival and proliferation in response to nutrient deprivation. *EMBO J.* **29,** 2082–2096
31. Bi, M., Naczki, C., Koritzinsky, M., Fels, D., Blais, J., Hu, N., Harding, H., Novoa, I., Varia, M., Raleigh, J., Scheuner, D., Kaufman, R. J., Bell, J., Ron, D., Wouters, B. G., and Koumenis, C. (2005) ER stress-regulated translation increases tolerance to extreme hypoxia and promotes tumor growth. *EMBO J.* **24,** 3470–3481
32. Dibner, C., and Schibler, U. (2015) Circadian timing of metabolism in animal models and humans. *J. Intern. Med.* **277,** 513–527